EUROPEAN ORGANIZATION FOR NUCLEAR RESEARCH

CERN-EP/80-229
23 December 1980

PRODUCTION OF CHARMED PARTICLES AT THE CERN INTERSECTING STORAGE RINGS IN EVENTS TRIGGERED BY AN ELECTRON

J. Irion[4], H. Seebrunner[4], M. Barone[2], M.M. Block[5], A. Böhm[1], R. Campanini[5*], F. Ceradini[2**], D. DiBitonto[3***], K.L. Giboni[1], D. Hanna[3***], H. Ludwig[5], F. Muller[2], B. Naroska[2†], F. Navach[4††], M. Nussbaum[2†††], C. Rubbia[2,3], D. Schinzel[2], A. Staude[4], R. Tirler[4] and R. Voss[4]

1) III. Physikalisches Institut d. Technischen Hochschule, Aachen, Germany
2) CERN, Geneva, Switzerland
3) Harvard University, Dept. of Physics, Cambridge, Mass., USA
4) Sektion Physik der Universität, Munich, Germany
5) Northwestern University, Evanston, Ill., USA

ABSTRACT

Production of charmed particles has been investigated at $\sqrt{s}$ = 63 GeV using the Lampshade Magnet detector triggered by electrons and positrons emitted at 30° from the ISR beam axis. The results of a search for Λ_c and $\bar{\Lambda}_c$ signals in the $K^-p\pi^+$ and $K^+\bar{p}\pi^-$ channels are presented. Cross-sections for the reactions $pp \to \bar{D}\Lambda_c X$ and $pp \to \Lambda_c\bar{\Lambda}_c X$, and upper limits for $pp \to D\bar{D}X$, are evaluated under various models and compared with other values obtained at the ISR.

(Submitted to Physics Letters)

---

* Now at the University of Bologna, Italy.
** Now at INFN, Sezione di Roma, Italy.
*** Now at CERN, Geneva, Switzerland.
† Now at DESY, Hamburg, Germany.
†† Now at the University of Bari, Italy.
††† Permanent address: University of Cincinnati, Ohio, USA.

The Lampshade Magnet detector at the CERN Intersecting Storage Rings (ISR) was used to study the processes

$$p + p \to X + \overline{C_1} + C_2 \begin{cases} \Lambda_c \to K^- p \pi^+ \\ D^+ \to K^- \pi^+ \pi^+ \end{cases}$$

and

$$p + p \to X + C_1 + \overline{C_2} \begin{cases} \bar{\Lambda}_c \to K^+ \bar{p} \pi^- \\ D^- \to K^+ \pi^- \pi^- \end{cases}$$

where $\overline{C_1}$ (C_1) is a particle of negative (positive) charm quantum number, the presence of which is signalled by a decay electron (positron). This investigation was part of a series of experiments using the same detector, the first of which [1], with a trigger favouring forward production, gave conclusive evidence for a Λ_c signal at $m(\Lambda_c) \simeq 2260$ MeV/c^2 in the $K^- p \pi^+$ channel.

The experimental set-up, shown in fig. 1, consisted of two magnetic spectrometers covering angular intervals of 14°-40° and 1°-6°. The outer spectrometer was built around an air-core toroidal magnet, the LSM. For electron identification, 10 of the sectors between the 12 thin coils were equipped with CO_2-filled Čerenkov counters (pion threshold $\sim$ 5 GeV/c) and lead/liquid scintillator shower counters effectively covering the 25°-35° angular range. The forward spectrometer used a septum dipole magnet; inside this, eight freon-filled Čerenkov counters allowed protons and kaons to be separated from pions (π, K, p thresholds: 2.6, 9.3, 17.7 GeV/c). Detailed descriptions of the track detectors (drift chambers for the LSM, proportional chambers for the dipole) have been published elsewhere [2,3]. The precision of measurement in this experiment was $\Delta p/p \sim 0.044p$ in the forward spectrometer, $\Delta p/p \sim 0.12p$ in the LSM for $p > 0.6$ GeV/c, which is the region of interest.

The main trigger selected events with one electron candidate and at least two other particles in the LSM. It required pulses in the trigger counters in front of any two sectors and, in addition, pulses in the trigger, Čerenkov, and shower counters of another sector (the shower counter pulse had to be above a threshold corresponding to $p_T \sim 0.4$ GeV/c for an electron).

The data collected with this electron trigger amounted to an effective integrated luminosity of $\sim 2.1 \times 10^{36}$ cm^{-2} at $\sqrt{s}$ = 63 GeV. For normalization purposes, the Čerenkov and shower counter requirements were dropped for part of the time so as to achieve a pion trigger of the same configuration as that of the electron trigger. To ensure equal acceptances for positive and negative particles, the LSM field was periodically reversed.

To enhance the prompt electron content of the trigger, software cuts on the pulse heights of trigger counters and Čerenkov counters were applied to reduce background from electron pairs and charged pion feedthrough; the energy deposited in the shower counter had to agree within errors ($\Delta E/E \sim 0.2/\sqrt{E}$) with the momentum calculated from track reconstruction. Thus there remained for analysis about 50,000 events with an $e^{\pm}$ candidate and three more tracks.

Charmed baryon (antibaryon) production was looked for in the channel $\Lambda_c \to K^- p \pi^+$ ($\bar{\Lambda}_c \to K^+ \bar{p} \pi^-$) in events where, according to the Čerenkov counter information, a positive (negative) particle in the forward arm was a proton (antiproton) candidate. Figure 2a shows the distribution of $K^- p \pi^+$ masses in events triggered by an e^-. It exhibits a sharp $\sim 3\sigma$ signal in the 2250-2270 MeV mass interval. The width of this peak is compatible with the mass resolution in this range ($\sigma \simeq 23$ MeV), and its location agrees with the former [1] measurement, using the same apparatus and the same decay channel, of the Λ_c^+ mass, m = 2262 ± 10 MeV [4]. An independent argument in favour of the Λ_c nature of this peak is that it does not appear in the $K^- p \pi^+$ spectra for events where the trigger particle was a π^- or an e^+ (figs. 2b and 2c).

Similarly, $K^+ \bar{p} \pi^-$ mass distributions are shown in figs. 2d, e, f when the trigger particle is an e^+, π^+, or e^-. A sharp $\sim 2\sigma$ blip in the Λ_c-region is seen in fig. 2d, whereas figs. 2e and 2f show no structure at this place. The signal is centred at a mass m $\sim$ 2245 ± 10 MeV (statistical), not incompatible with the location of the $K^- p \pi^+$ peak of fig. 2a. Actually the probability that the signal is due to a fluctuation of the background is lower than the probability for a mass m $\simeq$ 2260 MeV/c^2 to appear drifted down to the observed value; hence, with better than even odds, this peak may be interpreted as originating from $\bar{\Lambda}_c \to K^+ \bar{p} \pi^-$.

Production of $D^{\pm}$ mesons was also searched for, in the decay channel $D^{\pm} \to K^{\mp}\pi^{\pm}\pi^{\pm}$. In the analysis the K candidates were recognized by the $\check{C}$-counters in the forward arm. The mass spectra of the $K^{\mp}\pi^{\pm}\pi^{\pm}$ combinations obtained with $e^{\pm}$ triggers showed no enhancement in the D mass region.

For the Λ_c peak, the statistics allow a comparison of the Feynman x and p_T distributions inside the peak region with those in the neighbouring bins, which give the shape of the background distributions. In figs. 3a and 3b the experimental distributions of x and p_T of the Λ_c are displayed after subtraction of the background. Figure 3c shows the p_T spectrum of the triggering e^- associated with Λ_c. These spectra are of course not the true distributions at production, but are folded with the acceptance of the detector in momentum space.

This acceptance is calculated as follows. Particles C_1 and C_2 are generated in a correlated way, with different models*), yielding approximately for each of C_1 and C_2 the following production laws:

a) $d\sigma/dxd(p_T^2) \sim \exp(-bp_T^2)$ (flat x)

b) $d\sigma/dyd(p_T^2) \sim \exp(-bp_T^2)$ (flat y)

c) $Ed\sigma/dxd(p_T^2) \sim (1-x)^3 \exp(-bp_T^2)$ (central).

The electron from C_1 decay is emitted isotropically in C_1 c.m., with the experimentally measured [6] momentum spectrum, in the case $C_1 = D$. For $\Lambda_c\bar{\Lambda}_c$ production, the Λ_c decay is assumed to be half and half $\Lambda_c \to \Lambda_0 e^+\nu$ and $\Lambda_c \to \Sigma(1385)e^+\nu$, each one proceeding according to phase space. The hadrons from C_2 decay are also generated according to phase space.

---

*) The Feynman variable x of a subsystem containing particles C_1 and C_2 was generated according to either a) a diffractive distribution; b) a flat-x law, or c) a flat-y law. C_1 and C_2 were then attributed p_T^2 values generated from an $\exp(-bp_T^2)$ distribution and random x-values correlated by momentum conservation in the decay $S \to C_1\bar{C}_2$. This procedure yielded x_1 and x_2 distributions closely approaching a) flat-x laws, b) flat-y laws, c) central distributions $E(d\sigma/dx) \sim (1-x)^3$. In addition, for $\bar{D}\Lambda_c$ production, a model (a') was also used in which $d\sigma/dx(\Lambda_c) = c^t$ and $E(d\sigma/dx)(\bar{D}) \sim (1-x)^3$; asymmetrical production laws may be expected from mechanisms such as flavour excitation [5].

The acceptance w thus calculated is expected to be model-dependent. Actually, the acceptance for the hadrons from C_2 increases with increasing values of the Feynman x of C_2, whereas the acceptance (at $\sim 30°$) for the electron from C_1 is largest for small values of x (C_1). Thanks to this partial compensation, w decreases by only a factor of ~ 2 when going from model (a) to model (c); also, w depends only rather little on the value of the parameter b around its chosen value $b = 4\ GeV^{-2}$. On the other hand, as seen in fig. 3, the predicted x distribution of Λ_c's from the reaction $pp \to \bar{D}\Lambda_c\ldots$ is rather different for the various models, the data tending to rule out model (a).

Using the value of w calculated for a given reaction and model, the corresponding total cross-section σ (or its upper limit) is then given by

$$B_1 \cdot B_2 \sigma = \frac{N}{\mathcal{L}} \frac{1}{\varepsilon} \frac{1}{w} ,$$

where

N is the number of events deduced from the Λ_c and $\bar{\Lambda}_c$ mass peaks (or its 95% CL upper limit for D^+, D^- production);

$\mathcal{L} = 2.1 \times 10^6\ \mu b^{-1}$ is the integrated luminosity;

ε is the global efficiency for detection and reconstruction of the events, evaluated to be 0.065, with a 30% possible error resulting mainly from the uncertainty on track reconstruction efficiency in the LSM (0.57 ± 0.06), the other individual efficiencies being well measured;

B_1, B_2 are the branching ratios of particle C_1 ($\bar{C}_1$) into an e^+ (e^-), and particle $\bar{C}_2$ (C_2) into the observed hadronic final state: $B_1(D \to e\ \ldots) = 0.08$ [7], $B_2(\Lambda_c \to K^- p \pi^+) = 0.022$ [8], $B_2(D^+ \to K^- \pi^+ \pi^+) = 0.046$ [7].

The resulting cross-sections are shown in table 1, where the errors include only the statistical ones. For comparison with other experiments, the cross-sections for the reaction $pp \to D\Lambda_c X$ are calculated (line 1 of table 1) assuming that all observed Λ's (53 ± 20) come from this reaction*). They are of the same

*) Actually, if the $\bar{\Lambda}_c \to K^+ \bar{p} \pi^-$ signal (21 ± 15 events) is taken at face value and is assumed to originate from $pp \to \bar{\Lambda}_c \Lambda_c X$, then the same number of Λ_c's from that reaction should be present among the $\Lambda_c \to K^- p \pi^+$ events. This reduces the number of Λ_c's due to $pp \to \bar{D}\Lambda_c X$ from 53 ± 20 to 32 ± 25; the cross-sections of the first line should then be multiplied by 0.6 (and their errors by 1.25).

magnitude as the cross-sections obtained [9] by another ISR group in a comparable experiment (90° electron trigger) using similar models. This is illustrated in figs. 4a and 4b, which display the values of $d\sigma/dx$ and $d\sigma/dy$ from both experiments, using the corresponding models (a) or (a′) and (b). In addition, fig. 4 also gives the values obtained in former ISR experiments [4,10,11] in a region of generally higher values of x or y. There is no great disagreement between the various results (except for the high values from ref. 10), but they are not precise enough to decide against or for either the flat-x or flat-y assumptions.

Line 2 of table 1 gives for the various models the values of the $pp \to \bar{D}D^+ \ldots$ cross-section resulting from the 95% C.L. limits of the number of $(D^+ \to K^-\pi^+\pi^+)$ events associated with the e^- trigger. The upper limit for $d\sigma/dy$ obtained with model (b) is displayed in fig. 4c together with the corresponding value for $\bar{D}D^0$ from ref. 9 $(\bar{D} \to e^-,\ D^0 \to K^-\pi^+)$ and former ISR results on D^0 [4] or D^+ [4,12] production in the high-y region; again there is no apparent conflict between the data points.

Similarly, line 3 gives the upper limits for $pp \to D\overline{D^+} \ldots$ under the assumption that all possible $(\overline{D^+} \to K^+\pi^-\pi^-)$ events associated with an e^+ originate from $D\overline{D^+}$ production. These limits are higher than those of line 2 for the charge-symmetric final state $\bar{D}D^+$, giving room for the competing $\overline{D^+}$ production process: $pp \to (\Lambda_c \to e^+) + \overline{D^+} + \ldots$. Experimental upper limits for this process are given in line 4 of the table, calculated with the assumptions that all $(e^+)\cdot(K^+\pi^-\pi^-)$ events originate from $pp \to \Lambda_c\overline{D^+}X$ and that $B(\Lambda_c \to e^+) = 0.10$. These values should be compared with the cross-sections inferred from the observed final state $pp \to (\bar{D} \to e^-) + (\Lambda_c \to K^-p\pi^+) + X$; their values should be $\sim$ 30% of those given in line 1 of the table (assuming that $\overline{D^+}$ constitute 50% of the $\bar{D}$ and subtracting the $\sim$ 40% $\bar{\Lambda}_c\Lambda_c$ component). It can be seen that the cross-section values thus calculated are close to the upper limits given in line 4 of the table, which means that the value 0.1 represents (within large errors) an upper limit for the unknown branching ratio $B(\Lambda_c \to e^+)$.

Cross-sections for the reaction $pp \to \Lambda_c \bar{\Lambda}_c$ are given in the last line of table 1, assuming $B(\Lambda_c \to e^+) = 0.1$. For all models, they represent about 40% of the total Λ_c cross-sections (which remain close to those given by line 1), a ratio comparable to that found at the ISR [13] for the $\bar{\Lambda}^0/\Lambda^0$ ratio.

The results from this experiment thus look consistent with each other and with other ISR results on the production of (Λ_c, D^+, D^0) charmed particles identified by exclusive hadronic channels. The main positive result, derived from the observation of an $\sim 3\sigma$ Λ_c signal in association with electrons, is the largeness of the Λ_c production cross-section, whatever the model -- model (a'), the most favourable one, gives a lower limit of 160 μb at 95% C.L., including both the statistical error and the 30% uncertainty on detection efficiency (but not the $\sim$ 50% uncertainty on the $\Lambda_c \to K^- p \pi^+$ branching ratio from ref. 8). This result, by itself, is hardly compatible with <u>total</u> charm cross-section values from older ISR experiments on single electron [14,15] or $e^-\mu$ pair production [16,17] which were evaluated [18] *) to be of the order of 100 μb [15] or less [14,16,17]. The disagreement is of course even stronger if due allowance is made for D production, as observed [9] with a similar electron trigger.

Finally, it should be remarked that the popular gluon-fusion model [19] adjusted to fit σ(charm) $\sim$ 30 μb, as observed [20] at $\sqrt{s}$ = 27 GeV, predicts σ(charm) $\sim$ $\sim$ 100 μb at $\sqrt{s}$ = 63 GeV and a rapidly falling x-distribution. Other mechanisms should then be invoked [21] to account for the bigger cross-sections and wider x-distributions observed at the ISR.

We thank the ISR staff, particularly D. Coward, and our colleagues from Riverside, Cal., for their help in setting up and running this experiment. Discussions with B. Combridge and W. Geist are gratefully acknowledged, as well as the assistance of J.M. Perreau in solving computing problems. This work was supported in part by the US Department of Energy and by the Bundesministerium für Forschung und Technologie.

---

*) Under the assumption of central D-production (these experiments were rather insensitive to charm production outside the central region). The first indication for another mechanism came from the observatiom at the ISR [12] of abundant D^+ production at high x values.

REFERENCES

[1] K.L. Giboni et al., Phys. Lett. 85B (1979) 437.

[2] F. Ceradini et al., Nucl. Instrum. Methods 156 (1978) 171.

[3] L. Baksay et al., Nucl. Instrum. Methods 133 (1976) 219.

[4] J. Eickmeyer et al., Cross-sections for diffractive charm production at the CERN ISR, Submitted to the 20th Int. Conf. on High-Energy Physics, Madison, 1980.

[5] B.L. Combridge, Nucl. Phys. B151 (1979) 426.

[6] W. Bacino et al., Phys. Rev. Lett. 43 (1979) 1073.

[7] Average values from: G. Goldhaber and J.E. Wiss, Charmed mesons produced in e^+e^- annihilation, preprint LBL-10652 (1980).

[8] G.S. Abrams et al., Phys. Rev. Lett. 44 (1980) 10.

[9] G. Sajot, Communication to the 20th Int. Conf. on High-Energy Physics, Madison, 1980.

[10] W. Lockman et al., Phys. Lett. 85B (1979) 443.

[11] D. Drijard et al., Phys. Lett. 85B (1979) 452.

[12] D. Drijard et al., Phys. Lett. 81B (1979) 250.

[13] S. Ehran et al., Phys. Lett. 85B (1979) 441.

[14] F.W. Büsser et al., Nucl. Phys. B113 (1976) 189.

[15] M. Barone et al., Nucl. Phys. B132 (1978) 29.

[16] L. Baum et al., Phys. Lett. 77B (1978) 397.

[17] N. Chilingarov et al., Phys. Lett. 83B (1979) 136.

[18] W. Geist, preprint CERN-EP/79-78 (1979).

[19] C.E. Carlson and R. Suaya, Phys. Lett. 81B (1979) 329.

[20] S. Wojcicki, New flavour production, Rapporteur talk given at the 20th Int. Conf. on High-Energy Physics, Madison, 1980.

[21] See, for instance, R.J.N. Phillips, Phenomenology of new particle production, Rapporteur talk given at the 20th Int. Conf. on High-Energy Physics, Madison, 1980, and references therein.

Table 1

Cross-sections for various reactions and models

Final charmed state [a]		Number of events	σ (mb) [b]		
			Model a (a′)	Model b	Model c
$\bar{D} \to e^-$	$\Lambda_c \to K^- p \pi^+$	53 ± 20	1.22 ± 0.46 (0.84 ± 0.32)	1.65 ± 0.62	2.30 ± 0.87
$\bar{D} \to e^-$	$D^+ \to K^- \pi^+ \pi^+$	< 22	< 0.28	< 0.34	< 0.53
$D \to e^+$	$\overline{D^+} \to K^+ \pi^- \pi^-$	< 34	< 0.43	< 0.54	< 0.81
$\Lambda_c \to e^+$	$\overline{D^+} \to K^+ \pi^- \pi^-$	< 34	< 0.39	< 0.57	< 0.77
$\Lambda_c \to e^+$	$\bar{\Lambda}_c \to K^+ \bar{p} \pi^-$	21 ± 15	0.45 ± 0.32	0.67 ± 0.47	0.89 ± 0.62

a) The nature of the charmed particle in the first column is an assumption; only the e^- (or e^+) is observed.

b) The quoted errors do not include those on detection efficiency (±30%) nor on the branching ratios which have been measured elsewhere [7,8]. The unknown $\Lambda_c \to e^+$ branching ratio is assumed to be 0.1.

Figure captions

Fig. 1 : Experimental set-up.

Fig. 2 : $Kp\pi$ effective mass distributions, in 20 MeV/c^2 bins, for various trigger particles. The curves represent polynomial backgrounds, fitted outside the Λ_c region (plain curve); the error bars represent one standard deviation from the interpolated background (dotted) in the peak bin. The arrows show the location of the Λ_c peak, as seen in ref. 4.

Fig. 3 : a) x distribution of Λ_c events after subtraction of the background determined from the side bins.

b) p_T distribution of Λ_c events after subtraction of the background.

c) p_T distribution of the trigger electron for Λ_c events, after subtraction of the background.

The curves are the predictions of the models described in the text, taking into account the acceptance of the detector.

Fig. 4 : a) Experimental values of $d\sigma/dx$ for $pp \rightarrow \bar{D}\Lambda_c X$.

b) Experimental values of $d\sigma/dy$ for $pp \rightarrow \bar{D}\Lambda_c X$.

c) Experimental values of $d\sigma/dy$ for $pp \rightarrow \bar{D}(D^0 \text{ or } D^+)X$.

The values plotted have been calculated from the various references using the same branching ratios as in the present work. The points for refs. 9, 11, and 12 come from a recent updating by the authors (preliminary results communicated by W. Geist).

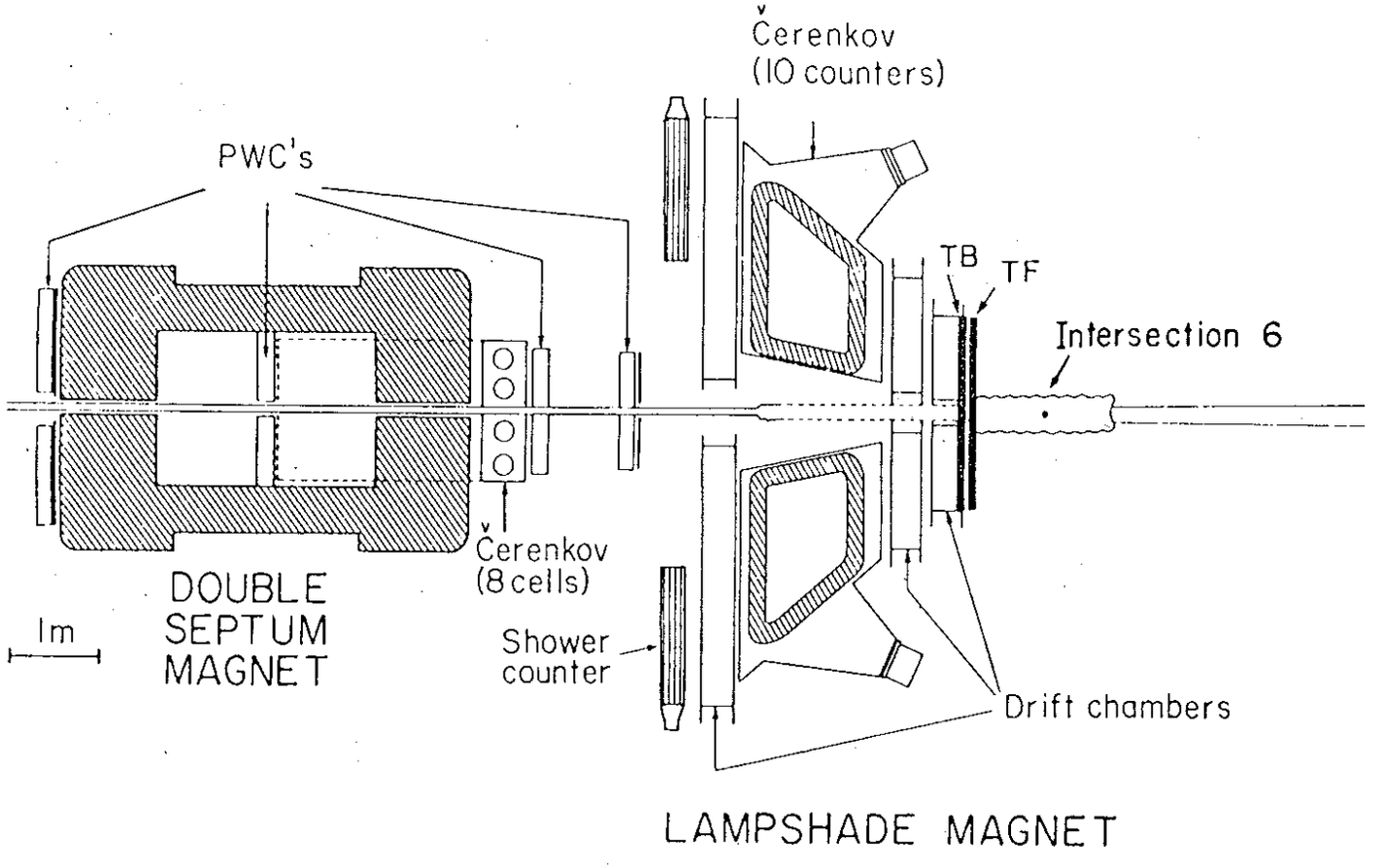
Čerenkov
(10 counters)
PWC's
TB
TF
Intersection 6
Čerenkov
(8 cells)
DOUBLE
SEPTUM
MAGNET
1m
Shower
counter
Drift chambers
LAMPSHADE MAGNET

Fig. 1

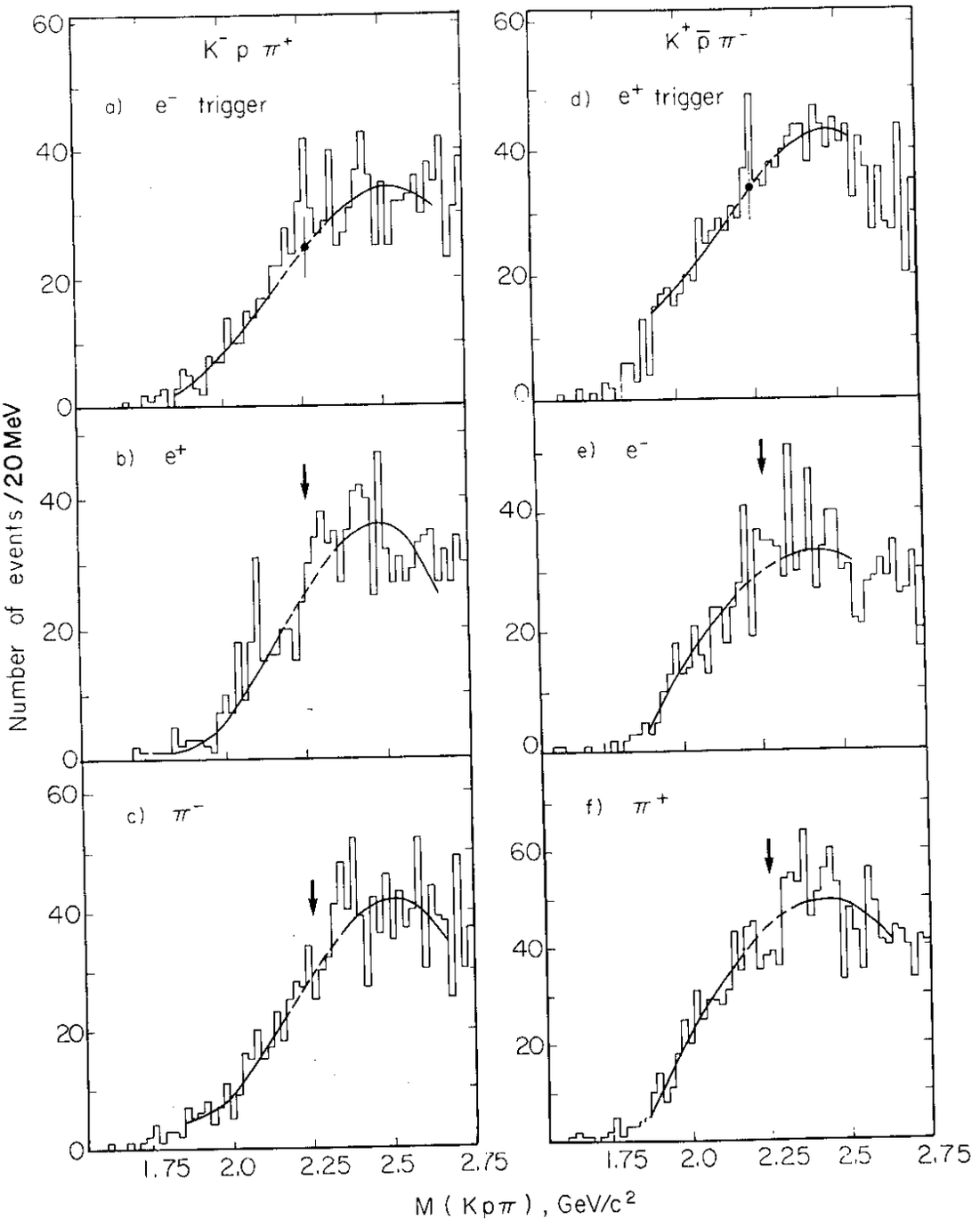
$K^- p \pi^+$
a) e^- trigger
b) e^+
c) π^-
$K^+ \bar{p} \pi^-$
d) e^+ trigger
e) e^-
f) π^+
Number of events / 20 MeV
M (Kpπ) , GeV/c²
1.75
2.0
2.25
2.5
2.75
0
20
40
60

Fig. 2

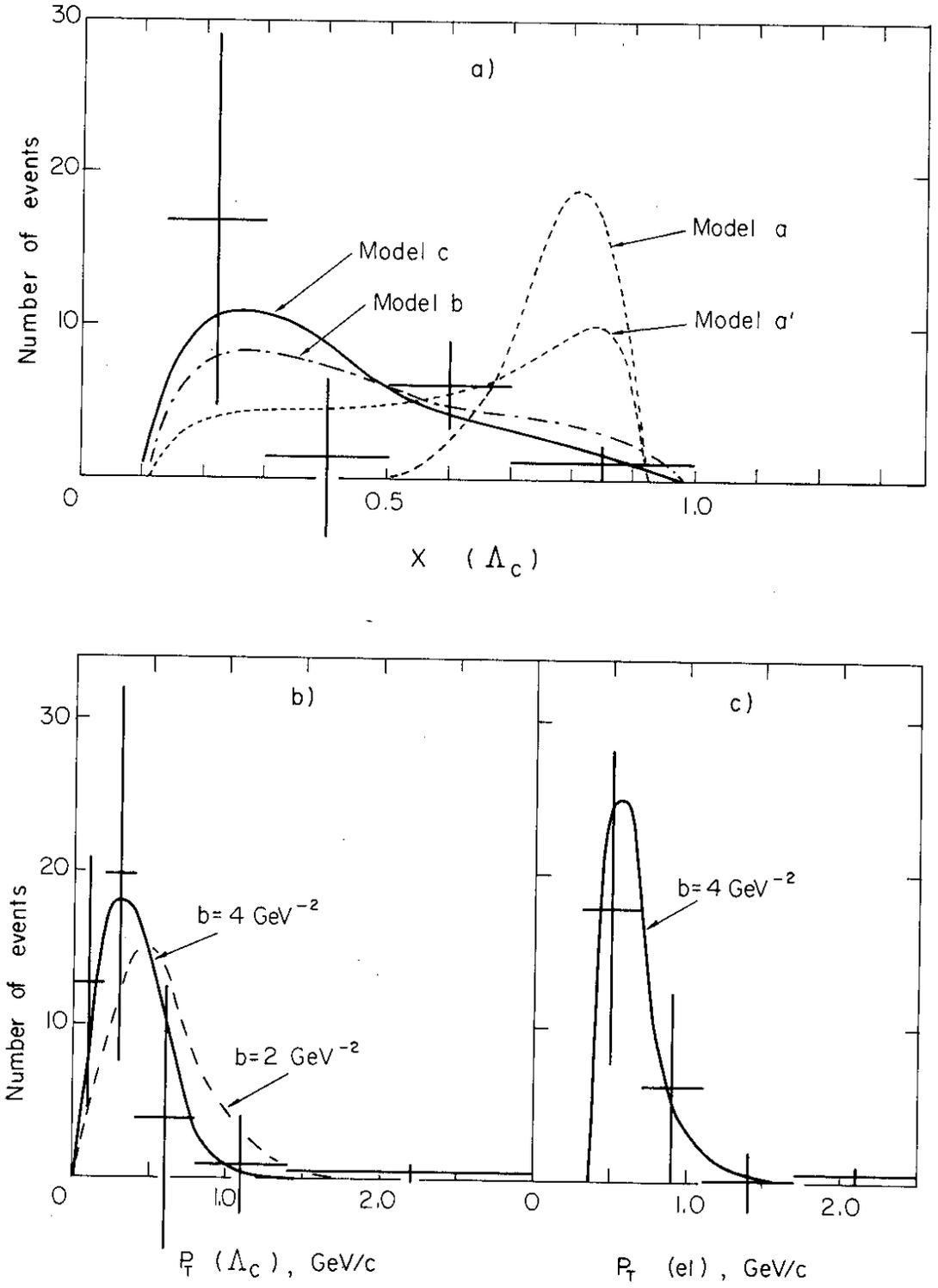
a)
Number of events
30
20
10
0
0.5
1.0
Model c
Model b
Model a
Model a'
X (Λ_c)
b)
c)
b= 4 GeV^{-2}
b= 2 GeV^{-2}
b= 4 GeV^{-2}
Number of events
30
20
10
0
1.0
2.0
0
1.0
2.0
P_T (Λ_c), GeV/c
P_T (el), GeV/c

Fig. 3

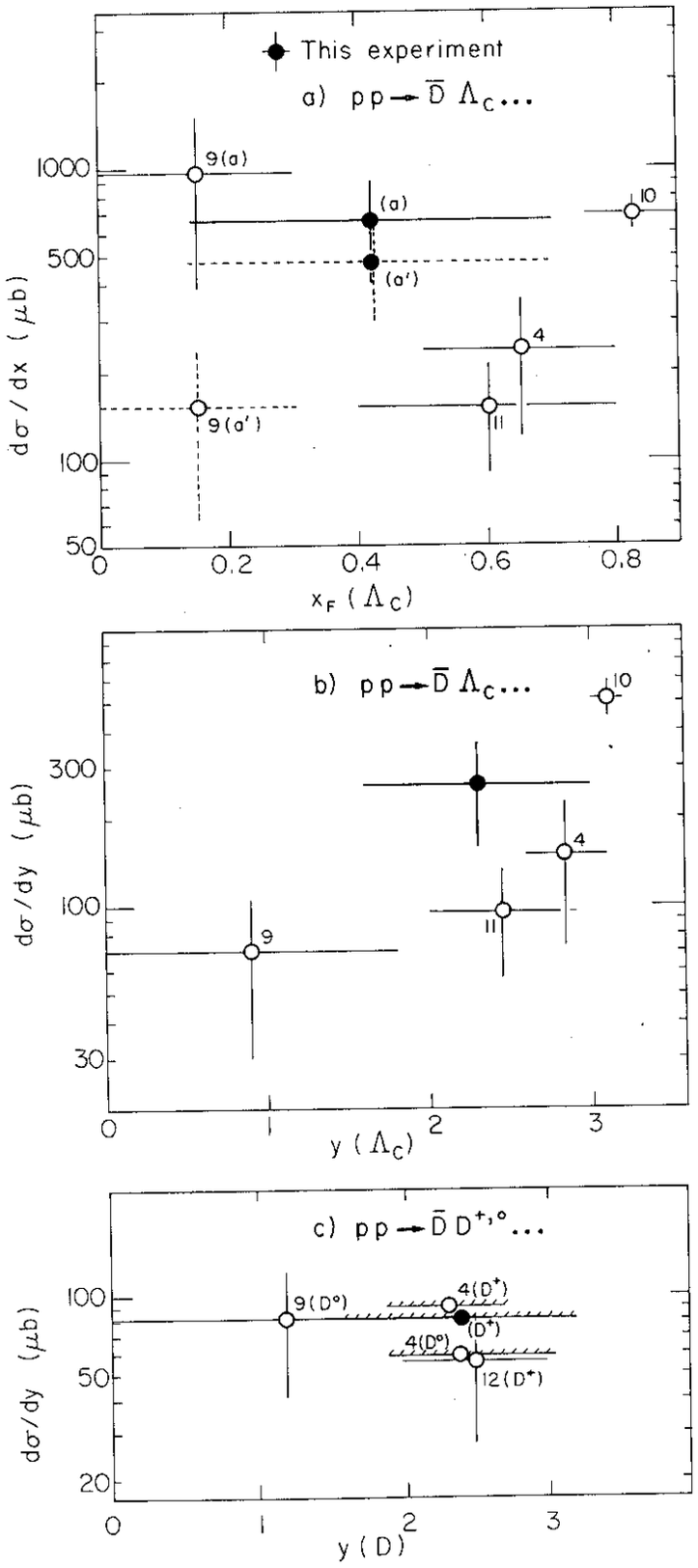
This experiment
a) pp → D̄ Λc...
9(a)
(a)
(a')
10
4
11
9(a')
1000
500
100
50
dσ / dx (μb)
0
0.2
0.4
0.6
0.8
xF (Λc)
b) pp → D̄ Λc...
10
4
11
9
300
100
30
dσ/dy (μb)
0
1
2
3
y (Λc)
c) pp → D̄ D+,°...
9(D°)
4(D+)
(D+)
4(D°)
12(D+)
100
50
20
dσ/dy (μb)
0
1
2
3
y (D)

Fig. 4